Articles

Metabolite Transfer via Enzyme-Enzyme Complexes

D. K. SRIVASTAVA AND SIDNEY A. BERNHARD

The concentrations of enzyme sites in cells are usually higher than the concentrations of cognate intermediary metabolites. Therefore metabolic pathways or substantial segments of pathways may proceed by the direct transfer of metabolites from one enzyme site to the next by means of enzyme-enzyme complex formation. This mechanism of metabolite transfer differs from that usually assumed where dissociation and random diffusion of metabolite through the aqueous environment is responsible for the transfer to the next enzyme site. Since the direct transfer mechanism does not involve the aqueous environment, the energetics of metabolite interconversion can differ from expectations based on aqueous solution data. Evidence is summarized suggesting that metabolite is transformed and transferred with equal facility everywhere in the direct transfer pathway.

THE PROPERTIES OF INDIVIDUAL ENZYMES ARE INFLUenced by interactions among enzymes, substrates, and solvent. Hence the concentrations of cellular components correspondingly affect the activity of the entire cellular milieu. Enzymological studies that focus primarily on the catalytic activity of individual enzymes are almost always performed under conditions far from physiological (*1*). This is largely a consequence of the high catalytic efficiency of enzymes. Measurements of substantial conversion of substrate to product at nanomolar concentrations of enzyme are possible over periods of several minutes. At nanomolar concentrations, functional effects of enzyme-enzyme interactions are in general not evident except for some stable multienzyme complexes. At the high concentrations of many enzymes in the cell, enzyme-enzyme interactions are far more likely. We first examine the intracellular concentrations of enzymes and their substrates (intermediary metabolites) and then discuss the functional consequences of potential enzyme-enzyme interactions.

Concentration of Enzymes and Metabolites in the Cell

It is generally assumed that metabolism proceeds by an abundant aqueous pool of metabolites that arrive at appropriate enzyme sites by free diffusion. At the enzyme sites metabolites are converted to products and finally dissociate to reenter the aqueous pool (*2–4*). In fact, the concentration of metabolites in the fluid (aqueous) regions of the cell are low when compared with the concentrations of their high affinity enzyme sites. The concentrations of enzyme sites in this cellular fluid are surprisingly high; in general, they exceed the concentration of their intermediary metabolites (*1, 5*). On the basis of the high affinity of enzymes for their specific metabolites, nearly all of the intermediary metabolites would be expected to be localized at their respective enzyme sites (Table 1) rather than uniformly dispersed in the aqueous environment. However, metabolites at the beginning and end of the pathways (precursors and final products) far exceed the concentration of their high affinity enzyme sites (*1*). The glycolytic metabolites fall into the two classes with respect to intracellular concentrations: (i) precursors and final products and (ii) intermediary metabolites.

In the case of glycolytic enzymes and their metabolites in muscle, the capacity of the enzymes for interaction with glycolytic intermediates is comparable to the total concentration of hexose phosphate (precursor) in the cell (Table 1). Hence, there is no a priori reason to expect that most of the precursor metabolites will be converted to final product (lactate) as would be the case in aqueous solution (*2, 6*) in the presence of minute quantities of the enzyme catalysts.

Although in this article we place particular emphasis on the glycolytic pathway of metabolism, there is reason to suspect that results and conclusions could extend to other metabolic pathways as well (*7–10*).

Physical Interactions Among Enzymes

It has been explicitly demonstrated that sequential pairs of enzymes in the tricarboxylic acid cycle form specific complexes (*1, 11, 12*). In some instances, complexes of enzymes containing more than one sequential pair have also been demonstrated (*1, 12*). At high concentrations of enzyme proteins, appropriate to both these experiments and to the physiological conditions, enzyme-enzyme interactions may be far more prevalent than previously envisaged (*1*).

In contrast to readily dissociable enzyme-enzyme complexes such as tricarboxylic acid cycle enzyme complexes mentioned above, other stoichiometric enzyme complexes known as multienzyme systems exist that are more stable (*13–15*). The existence of these multienzyme complexes suggests that their interactions have a functional role in the overall reaction processes; this relation has been explicitly demonstrated in the case of the two-enzyme complex tryptophan synthase (*16*).

Interactive enzymes and multienzyme complexes may represent arbitrary distinctions in the strength of the enzyme-enzyme interactions (*13*). For example, the enzymes of fatty acid synthesis (fatty acid synthase) are all covalently linked into a large polypeptide in the mammalian multienzyme system. In yeast, six enzymes of fatty acid

D. K. Srivastava is a senior research associate in the Institute of Molecular Biology and S. A. Bernhard is a professor of chemistry and a member of the Institute of Molecular Biology, University of Oregon, Eugene, OR 97403.

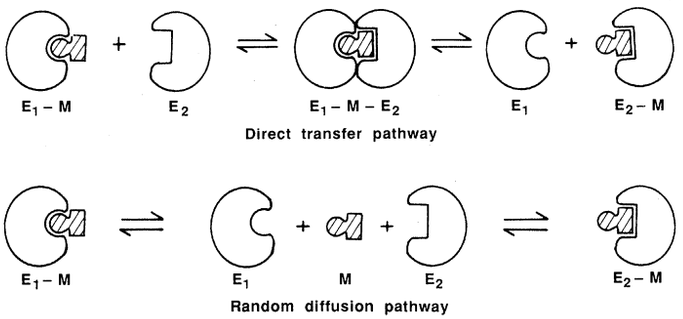

Fig. 1. Schematic representation of the mode of transfers of metabolite (M) between two sequential enzyme sites (E_1 and E_2). In direct transfer mechanism, metabolite (M) does not dissociate from E_1 to reach at the E_2 site. This is in contrast to the random diffusion mechanism in which metabolite (M) dissociates from E_1 into aqueous solvent before forming a complex with E_2.

synthase are covalently linked into two different sets of polypeptide chains. In prokaryotes and plants, the enzymes are noncovalently linked, and are readily separable from each other by standard nondenaturing chromatographic procedures (*17–20*). Nevertheless, the mechanism of fatty acid chain elongation is the same, and the individual enzymes are virtually the same in all of these systems (*17*).

Whereas functional channeling in the case of the multienzyme systems has been explicitly proposed many times, the functional interactions among sequential globular enzymes have received less attention (*1, 10, 11*). Because of the high intracellular concentration of proteins, such interactions are far more likely in vivo than has been evident from enzymological experiments in vitro at low protein concentrations (*5, 21*).

We have assembled experimental evidence for the direct transfer of metabolites (channeling possibly) among sequential pairs of enzymes via the formation of enzyme-enzyme complexes. Such direct transfers have functional advantages over transfers via the aqueous environment, which are described and discussed below.

Direct Transfer of Metabolites by Enzyme-Enzyme Complexes

The idea that metabolites can be transferred from one enzyme site to another without the intervention of the external solvent environment is not novel. Considerable evidence for the channeling of metabolites through a segment of a pathway has been assembled (*10*). The early evidence is based largely on two types of experiments: (i) the inability of metabolic intermediates to compete with precursor in the formation of final product; and (ii) the inability of a specific enzyme to utilize metabolic precursor synthesized by one of a diverse pair of enzyme pathways (*1, 10*), for example, the inability of ornithine transcarbamylase to utilize carbamyl phosphate synthesized via the glutamine-dependent carbamyl phosphate synthase (*22*).

More explicit evidence for the involvement of enzyme-enzyme complexes in the transfer of metabolite (Fig. 1) came from kinetic experiments by Cori *et al.* (*23*) and by Nygaard and Rutter (*24*). Although Cori *et al.* and Nygaard and Rutter had demonstrated direct metabolite transfer between enzymes, the experiments have only recently been appreciated (*25*). In part, this oversight must stem from the subsequent quantitative demonstrations of the high efficiency of individual enzyme catalysis, and from the lack of indications of protein-protein interactions at concentrations of protein sufficient to conduct facile enzyme kinetic experiments. Indeed, one might ask why such direct transfer mechanisms would be of consequence when the individual enzymes operate so efficiently? More recent experimental evidence from our laboratory supports the direct transfer mechanism (*1*).

We first recognized that something other than the usually assumed dissociation-random diffusion mechanism (Fig. 1) was appropriate to understand the coupled reactions catalyzed by phosphoglycerate kinase (PGK) and glyceraldehyde-3-phosphate dehydrogenase (GPDH). These reactions involve the initial conversion of 3-phosphoglycerate (3PGA) and adenosine triphosphate (ATP) to diphosphoglycerate (DPG) and adenosine diphosphate (ADP) followed by the reaction of DPG with reduced nicotinamide adenine dinucleotide (NADH) to form glyceraldehyde-3-phosphate (G-3-P), oxidized nicotinamide adenine dinucleotide (NAD^+) and phosphate (P_i)

$$3PGA + ATP \overset{PGK}{\rightleftharpoons} DPG + ADP \xrightarrow[NADH]{GPDH} NAD^+ + G\text{-}3\text{-}P + P_i \quad (1)$$

From ^{32}P nuclear magnetic resonance (NMR) studies, it was concluded that the binding of the substrate, diphosphoglycerate, to the enzyme phosphoglycerate kinase was extremely tight. This is apparent from the slow rotational relaxation of the phosphorus NMR signal resulting from its complex formation with the large protein molecule (*26–28*). This slow relaxation permits a calculation of a maximal rate of dissociation of the substrate from the enzyme to the aqueous environment with a specific rate of 1 per second.

The coupled reactions shown in Eq. 1 are widely utilized for measurement of ATP concentration since NADH disappearance is easily measurable. If the enzyme glyceraldehyde-3-phosphate dehydrogenase is used in large excess over that of phosphoglycerate kinase, the coupled reaction process reaches a limiting fast rate. According to the NMR measurements of the rate of diphosphogly-

Table 1. Concentration of enzymes and metabolites of glycolytic pathway. Values adapted or recalculated from the available data (*1*).

Pathway item	Concentration (μM)	k_{cat}* (sec^{-1})
Enzymes		
Phosphoglucomutase	31.9	250
Aldolase	809.3	15
α-Glycerol-P-dehydrogenase	61.4	100
Triose-P-isomerase	223.8	5000
Glyceraldehyde-3-P-dehydrogenase	1398.6	50
Phosphoglycerate kinase	133.6	700
Phosphoglycerate mutase	235.9	200
Enolase	540.7	40
Pyruvate kinase	172.9	300
Lactate dehydrogenase	296.0	600
Metabolite precursors and products		
Glucose-6-phosphate	3900	
Fructose-6-phosphate	1500	
Lactate	3700	
ATP	8050	
Inorganic phosphate	8000	
Metabolite intermediates		
Fructose-1,6-diphosphate	80	
Dihydroxyacetone phosphate	160	
Glyceraldehyde-3-phosphate	80	
1,3-Diphosphoglycerate	50	
3-Phosphoglycerate	200	
2-Phosphoglycerate	20	
Phosphoenol pyruvate	65	
Pyruvate	380	
NAD^+	541	
NADH	50	

*Approximate value at physiological *p*H, which we determined or recalculated from available data of others.

Table 2. Comparison of the rates of E_2-catalyzed reduction of its specific substrate (S_2) by NADH in the presence of E_1, with those predicted on the basis of free NADH as the only competent coenzyme. In 50 m*M* tris-HCl buffer, *p*H 7.5, containing 0.35 m*M* 2-mercaptoethanol and 1 m*M* EDTA unless specifically stated otherwise.

E_1	[E_1-site] (μM)	[NADH] (μM)	E_2	[E_2] (nM)	Rate (μM/min)		Stereochemistry	
					Predicted*	Observed	E_1	E_2
GPDH	220.0	134.0	LDH	0.029	0.17	1.05	B	A
LDH	170.0	49.5	GPDH	0.108	0.02	0.52	A	B
LDH	141.0	32.6	αGDH	0.138	0.03	0.32	A	B
GPDH	47.0	22.5	αGDH	0.211	0.24	0.24	B	B
αGDH	67.0	49.5	GPDH	0.108	0.23	0.16	B	B
αGDH	168.7	35.8	LDH	0.032	0.02	0.10	B	A
GPDH	104.1	16.7	LADH†	0.56	0.03	0.88	B	A
LADH	41.0	24.4	LDH	0.02	0.08	0.08	A	A
LDH	168.7	38.6	LADH	0.45	0.08	0.08	A	A

*Based on the aqueous NADH concentration, calculated from the appropriate dissociation constants of E_1-NADH and kinetic parameters for the E_2-catalyzed reaction (*1, 25, 31*). †Experiments with liver alcohol dehydrogenase (LADH) were carried out in 50 m*M* pyrophosphate buffer (*25*).

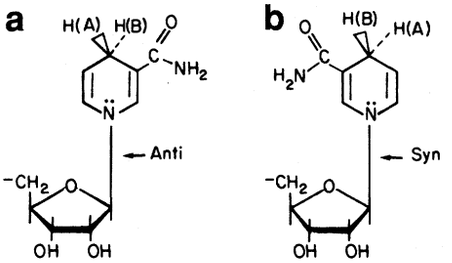

Fig. 2. The anti (a) and syn (b) conformation of NADH when bound to A and B dehydrogenases, respectively. The chirality of the hydrogens [H(A) and H(B))] at C-4 are shown for both conformations.

cerate desorption from the kinase enzyme, this rate cannot be faster than 1 per second per kinase molecule. In actuality, the coupled reaction velocity is more than 500 molecules of diphosphoglycerate reacted per kinase molecule, a rate nearly three orders of magnitude in excess of the predicted maximal desorption rate (*29*). Thus, in the case of this coupled reaction pathway, the mechanism cannot involve the dissociation of common intermediate (diphosphoglycerate) into the aqueous medium and its diffusion to the second enzyme site (*30*).

In a set of kinetic experiments designed to probe the order of molecular events, we have demonstrated that the pathway of transfer of diphosphoglycerate between phosphoglycerate kinase and glyceraldehyde-3-phosphate dehyrogenase is entirely consistent with a simple direct transfer mechanism and inconsistent with the conventionally assumed dissociation-diffusion mechanism (Fig. 1) (*30*). The experimental results demonstrate that the phosphoglycerate kinase–diphosphoglycerate complex is in itself a competent substrate for the reaction catalyzed by glyceraldehyde-3-phosphate dehydrogenase (*30*).

The specific rate of dissociation of diphosphoglycerate from phosphoglycerate kinase is unusually slow. In general, the rate of dissociation of reactants and products is comparable to or larger than the rates at which substrates are converted to products at the catalytic sites of enzymes. Hence, no qualitative conclusions regarding mechanistic pathway are generally discernible from the magnitudes of catalytic turnover numbers for coupled reaction processes (*25*).

It is well established that individual enzyme-catalyzed reactions, studied under optimal environmental conditions, show a hyperbolic dependence of reaction velocity on metabolite (M) concentration. The dependence of reaction velocity (v) on metabolite concentration is formulated by Michaelis-Menten equation (Eq. 2); E, M, and P are enzyme, metabolite, and final product, respectively; K_m is the affinity of enzyme for metabolite (M), and k_{cat} is the first-order rate constant for the conversion of enzyme-metabolite complex (E-M) to enzyme (E) and product (P).

$$E + M \underset{K_m}{\rightleftharpoons} E - M \xrightarrow{k_{cat}} E + P \qquad (2)$$

$$V = \frac{k_{cat} \times [E]_t}{1 + (K_m/[M])} = \frac{V_{max}}{1 + (K_m/[M])}$$

The affinity parameter (K_m) derived for most of the enzyme-catalyzed reactions that we discuss is of the order of 1 μM to 100 μM. When the substrate concentration is substantially less than the K_m, the reaction velocity will be likewise substantially below the saturated maximal value (V_{max}). In order to probe for the direct transfer mechanism with such enzymes, it becomes necessary to substantially buffer the aqueous common metabolite concentration to a very low value (*25*). This can be achieved if high concentrations of a high affinity enzyme site (E_1) are realizable. Under such conditions, the aqueous concentration of a common metabolite can be reduced to values far below that of K_m for an E_2-catalyzed reaction (*25*). In this way, the E_1-metabolite complex can be distinguished from the aqueous metabolite as a competent substrate for the E_2-catalyzed reaction (*25, 31*). For example, consider a dehydrogenase (E_2)-catalyzed oxidation of NADH. In the presence of a large excess of another dehydrogenase (E_1), the aqueous concentration of NADH can be severely lowered. Under such conditions, the NADH-dependent reaction catalyzed by E_2 can be reduced to a predictably very slow rate if aqueous NADH is the only competent substrate (*25, 31*). The predicted E_2-catalyzed reaction velocity in the presence of E_1 and M (based on the assumption that aqueous NADH is the only competent reductant) is compared with the experimental value shown in Table 2. Sometimes experimental results and calculated prediction agree quite precisely, but in other cases the experimental velocity is much greater than that predicted according to the dissociation-diffusion mechanism (Fig. 1). In the latter cases, the complex E_1-NADH must itself be a competent substrate for the E_2-catalyzed reaction, and hence the coupled reaction process must involve metabolite transfer via an intermediate E_1-E_2 complex.

Enzyme-Enzyme Complex Formation

In all cases where the direct transfer mechanism can be demonstrated by the methods outlined above, a second phenomenon is generally observable. At higher concentrations of the complexed common metabolite, such as E_1-NADH, a limiting velocity is reached for the rate of the E_2-catalyzed reaction. The E_2-catalyzed reaction velocity depends on E_1-NADH concentration in a hyperbolic or Michaelian fashion. This implies a saturation of the limiting E_2 molecules with E_1-NADH, and hence the formation of a substantial amount of enzyme-enzyme complexes (*25, 31*). The saturation in E_2-catalyzed reaction velocity with E_1-M concentration occurs not only with coupled reactions involving dehydrogenases but with other reactions as well (*1*). In all cases, where E_1-M is a competent substrate for the E_2-catalyzed reaction, we have demon-

Table 3. Values of K_m and k_{cat} for the E_2-catalyzed reaction with E_1-M as a competent metabolite substrate (*1, 30, 31, 35*); DHAP, dehydroxyacetone phosphate.

Complex (E_1-M)	E_2	$K_m^{(E_1\text{-}M)}$ (μM)
GPDH-NADH	LDH	5.88 ± 1.21
LDH-NADH	GPDH	2.60 ± 0.45
LDH-NADH	αGDH	1.21 ± 0.36
PGK*-DPG	GPDH	12.00 ± 2.00
Aldolase-DHAP	αGDH	8.00 ± 4.00
GPDH†-NAD^+	LDH	~10.00

*In 50 m*M* 2-methylimidazole buffer, *p*H 7.4. †In 100 m*M* glycine buffer, *p*H 9.0, containing 0.35 m*M* 2-mercaptoethanol and 1 m*M* EDTA.

strated a Michaelian relation between reaction velocity and E_1-M concentration.

Among the enzyme-enzyme interactions summarized in Table 3, the interactions among dehydrogenases are particularly noteworthy because of the extensive utilization of NADH (and NADPH) as a specific coenzyme substrate in many enzyme-catalyzed reactions (*32*). On the basis of many kinetic experiments of the type described above, involving a diversity of dehydrogenases, we have discerned a general rule for the applicability of the direct transfer mechanism (*31*). Direct transfer will occur whenever the two dehydrogenases exert opposite chiral specificity for the transfer of hydrogen between the C-4 of the nicotinamide ring and the substrate (Fig. 2). The two classes of dehydrogenases have been designated as A and B (*32, 33*). Direct transfer of coenzyme occurs between any A-B pair of dehydrogenases but does not occur between two A or two B dehydrogenases (Table 2) (*31*).

From the molecular graphic analyses of three dehydrogenases of known structure, we have proposed a molecular mechanism for the direct transfer of coenzyme between A and B dehydrogenases based on two specific structural details. (i) The different conformations of coenzyme in A dehydrogenase (anti; Fig. 2a) compared to B dehydrogenase (syn; Fig. 2b) leads to a nonmirror image relation between chiral coenzyme molecules when two enzymes of opposite chiral specificities are juxtaposed cleft to cleft (*34*). For this reason, it is possible to transfer the nicotinamide ring from site A to site B (or vice versa) without permitting internal molecular rotation, a process that is restricted at the enzyme surface but occurs readily and rapidly in the aqueous solvent. (ii) In the limited instances where we have had the opportunity to examine the three-dimensional structural coordinates, the molecular surface surrounding the active site cleft of the A dehydrogenases (for example, liver alcohol dehydrogenase and lactate dehydrogenase) is virtually entirely negatively charged, whereas the complementary molecular surface in a B dehydrogenase (such as glyceraldehyde-3-phosphate dehydrogenase) is entirely positively charged (*34*). These surrounding surfaces are each sufficiently charged such that A-A or B-B interactions would lead to strong repulsions.

Although the steady-state kinetic methods described above are adequate to demonstrate the direct transfer pathway, they do not indicate the details of the transfer mechanism. This is an inherent failing of the steady-state kinetic approach. Since many turnovers of substrate are required for quantitative interpretation of the steady-state data, there are almost no details available as to events within a single cycle of enzyme-catalyzed reaction. Such information is obtainable from transient reaction methods.

The generality of the direct transfer mechanism for the transfer of NADH between any A-B pair of dehydrogenases provides an opportunity to observe the transfer of NADH among different enzymes (*1, 31*). This transfer process can be visualized experimentally because of the difference in absorption or fluorescence emission spectra of NADH when bound in the anti versus syn conformation (*35, 36*). The transfer of NADH from E_1-NADH to an excess of E_2 follows a single exponential rate law. Remarkably, at sufficiently high concentrations of E_2, the single exponential transfer rate constant (k_{trans}) becomes independent of the particular E_2 concentration. At equilibrium, NADH is distributed nearly equally between E_1 and E_2 sites. Specific rate constants (k_{trans}) under conditions of E_2-saturation are listed in Table 4. There is a near uniformity in magnitudes of the rate constants, and the rate constants are nearly independent of the specific donor and acceptor enzymes and of whether coenzyme transfer is from A to B or from B to A.

This finding of nearly equal coenzyme transfer rates (k_{trans}) is consistent with the equilibrium distribution of NADH between E_A and E_B sites in equilibrium mixtures of E_A and E_B. This equilibrium distribution has been explicitly determined in the case of one A-B pair, namely, α-glycerol-phosphate dehydrogenase (αGDH) and lactate dehydrogenase (LDH) (*35*). Starting with NADH and an excess of α-glycerol-phosphate dehydrogenase, a titration was carried out with the cognate A enzyme lactate dehydrogenase. As the concentration of lactate dehydrogenase is increased, there is a progressive shift of the NADH spectrum from that characteristic of the syn conformation to that for the anti conformation. At higher concentrations of lactate dehydrogenase (higher than that of α-glycerol-phosphate dehydrogenase), the spectral shift reaches a maximal value. At this saturated level, the observed spectrum is a composite of nearly equal contributions of syn and anti NADH, indicating a nearly equal distribution of NADH between the two sites. Further increases in the concentration of lactate dehydrogenase reveal no further tendency toward formation of anti conformation at the lactate dehydrogenase (A enzyme) site. This finding indicates a strong affinity for NADH binding within the E_A-E_B complex compared to binding of the coenzyme to either individual enzyme (*35*). Because of the already high concentrations of the two enzymes in these experiments, it is not possible to increase the excessive lactate dehydrogenase concentration. Presumably, at sufficiently high concentrations of lactate dehydrogenase, all of the coenzyme would be bound to lactate dehydrogenase in the anti conformation. In any event, this equilibrium titration result and the saturation in magnitude of the rate constant for coenzyme transfer at high E_2 concentrations (Table 4) indicate the formation of a tight E_1-NADH-E_2 complex.

Modulation of the Facility for Ligand Transfer

The nearly equal specific rates of coenzyme transfer (k_{trans}) are in contrast to the considerably variable specific rates of coenzyme dissociation (k_{off}) from individual enzymes (*35*). These dissociation rate constants (k_{off}) vary by over a range of nearly two orders of magnitude (*35*). It is interesting that the nearly constant transfer rates lie in between the extremes of rates for coenzyme dissociation from the individual enzymes. The interactions between the pairs of A-B dehydrogenases thus appear to modulate the dissociation and transfer of coenzyme from one site to the other within the complex.

This modulation is further emphasized by the two experiments illustrated in Fig. 3. In each of these stopped-flow transfer experiments, NADH transfer is being monitored from a B enzyme carrier to an A enzyme acceptor. The two experiments differ in that the specific rates of dissociation (k_{off}) of NADH from the two B dehydrogenase sites (α-glycerol-phosphate dehydrogenase and glyceraldehyde-3-phosphate dehydrogenase) are at extreme limits of magnitude (*35*); for α-glycerol-phosphate dehydrogenase k_{off} is 9.0 sec^{-1} whereas for glyceraldehyde-3-phosphate dehydrogenase k_{off} is

Table 4. Transient relaxation rate constants (k_{trans}) for the transfer of NADH from E_1 to E_2. The stopped-flow spectrofluorometer was used to measure the changes in fluorescence intensity of NADH due to the ligation at A versus B dehydrogenases.

E_1*	E_2	k_{trans} (sec^{-1})
αGDH	LDH	142 ± 21
LDH	αGDH	172 ± 22
LDH	GPDH	180 ± 25
GPDH	LDH	232 ± 28

*Equal volumes of solution A (E_1-NADH) and solution B (E_2) were mixed at 0 time (E_1 > NADH < E_2). The fluorescence intensity of the mixture was monitored as a function of time. Fluorescence excitation wavelengths were 340 nm and 360 nm for GPDH-LDH and αGDH-LDH pairs, respectively. The fluorescence emission spectrum in each case was filtered through a 408-nm cutoff filter (*35*).

>350 sec^{-1}. Nevertheless, the specific rate constants of transfer (k_{trans}) of NADH from the two B dehydrogenases to lactate dehydrogenase are nearly equal; that is, in Fig. 3, curve 1b, k_{trans} is 163 sec^{-1} and in Fig. 3, curve 2b, k_{trans} is 204 sec^{-1}. The rate of dissociation of NADH from α-glycerol-phosphate dehydrogenase in the presence of bound lactate dehydrogenase has been strikingly enhanced, whereas the rate of dissociation of NADH from glyceraldehyde-3-phosphate dehydrogenase in the presence of bound lactate dehydrogenase has been decreased as a consequence of enzyme-enzyme interaction.

The equal facility for metabolite transfer between two sequential enzymes is not restricted to NADH transfer among dehydrogenases. The facility for the transfer of the common metabolite, diphosphoglycerate between glyceraldehyde-3-phosphate dehydrogenase and phosphoglycerate kinase proceeds with nearly equal facility in both directions. Even at concentrations of one of the two enzymes in large excess over the other, the equilibrium distribution of bound diphosphoglycerate is nearly equal between the two enzyme sites (*37*).

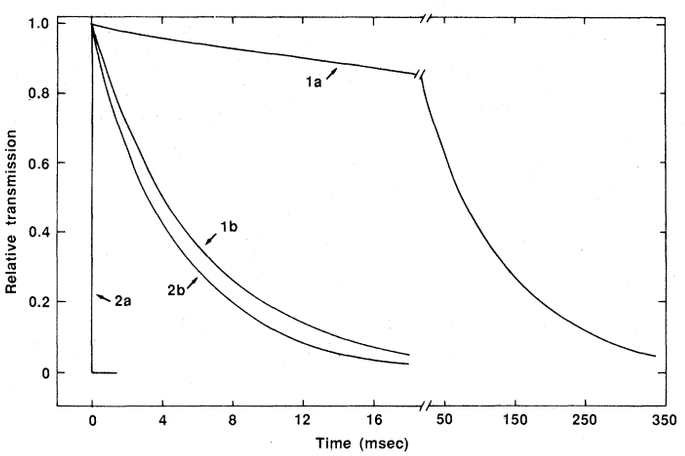

Fig. 3. Transient rates of NADH transfer. The rates of NADH transfer from αGDH and GPDH to LDH (k_{trans}) are compared with the specific rates of NADH dissociation (k_{off}) from αGDH and GPDH, respectively. These stopped-flow experiments were carried out by monitoring the fluorescence changes at wavelengths greater than 408 nm (*35*). Equal volumes of solution A and solution B were mixed at 0 time. Fluorescence intensity of the mixture was monitored as a function of time. Reaction, configuration, and experimental conditions are shown for each curve. Curve 1a: αGDH-NADH + $NAD^+ \xrightarrow{k_{off}}$ αGDH-NAD^+ + NADH [αGDH (18.6 μ*M* site), NADH (12.3 μ*M*) (solution A) + NAD^+ (20 m*M*) (solution B), excitation at 340 nm, k_{off} = 8.6 sec^{-1}]. Curve 1b: αGDH-NADH + LDH $\xrightarrow{k_{trans}}$ αGDH + LDH-NADH [αGDH (16.6 μ*M* site), NADH (10.8 μ*M*) (solution A) + LDH (43.2 μ*M* site) (solution B), excitation at 360 nm, k_{trans} = 163 sec^{-1}]. Curve 2a: GPDH-NADH + $NAD^+ \xrightarrow{k_{off}}$ GPDH-NAD^+ + NADH [GPDH (18.2 μ*M* site), NADH (12.0 μ*M*) (solution A) + NAD^+ (15 m*M*) (solution B), excitation at 295 nm, k_{off} >350 sec^{-1}]. Curve 2b: GPDH-NADH + LDH $\xrightarrow{k_{trans}}$ GPDH + LDH-NADH [GPDH (14.6 μ*M* site), NADH (10.8 μ*M*) (solution A) + LDH (40.8 μ*M* site) (solution B), excitation at 340 nm, k_{trans} = 204 sec^{-1}].

Not only is there equal facility for coenzyme transfer among dehydrogenases, but the distribution of reactive substrate and product complexes at an individual dehydrogenase site (K_{eq}^{int}) is again near unity (*1, 38*). Thus for example, the distribution of reactants and products in the reduction of pyruvate by NADH, catalyzed by lactate dehydrogenase (Eq. 3) is near unity (K_{eq}^{int} = 1).

$$\text{NADH} + \text{pyruvate} + \text{H}^+ \overset{\text{LDH}}{\rightleftharpoons} \text{LDH}\begin{matrix}\diagup \text{NADH} \\ \diagdown \text{pyruvate}\end{matrix} \rightleftharpoons \text{LDH}\begin{matrix}\diagup \text{NAD}^+ \\ \diagdown \text{lactate}\end{matrix} \overset{\text{LDH}}{\rightleftharpoons} \text{NAD}^+ + \text{lactate} \quad (3)$$

Reactants and products are comparably distributed among the lactate dehydrogenase site and, in the presence of α-glycerol-phosphate dehydrogenase, the NADH is comparably distributed between the lactate dehydrogenase and α-glycerol-phosphate dehydrogenase sites.

This partitioning of reactants and products is not surprising since there is already evidence for equipartitioning between reactants and products at a variety of different enzyme sites (*1, 38*). These internal equilibrium constants near unity are very often in contrast with the magnitudes of the equilibrium constants for the same reactions in aqueous solution (*1, 38*).

The resultant internal equilibrium constant near unity has been postulated to arise from an evolutionary drive toward optimally efficient catalysis (*38, 39*). We present below arguments that facile direct transfer of metabolites, rather than maximal catalytic velocity, may be the significant selective evolutionary feature for maintaining the internal equilibrium constants near unity.

Functional Consequences of the Direct Transfer Pathway

It is possible that the equal facility for metabolite transfer between cognate or sequential enzymes, a phenomenon which cannot be attributed to identical structural features within the two cognate enzymes, may be a feature that has evolutionary advantage. If so, this selected feature can lead to the observed equipartition of reactants and products within the individual enzyme sites. There is equal facility for diphosphoglycerate transfer between glyceraldehyde-3-phosphate dehydrogenase and phosphoglycerate kinase, as well as the equipartition of reactants and products within the phosphoglycerate kinase site (*26, 28*). The equilibrium constant near unity for metabolite transfer between glyceraldehyde-3-phosphate dehydrogenase and phosphoglycerate kinase is in contrast to that observed for distribution of the metabolite (diphosphoglycerate) between glyceraldehyde-3-phosphate and aqueous solvent (*37*). The near equal rates of metabolite transfer in the forward and reverse directions between glyceraldehyde-3-phosphate and phosphoglycerate kinase add further argument that this (evolutionary) drive is toward equally facile metabolite transfer between sequential enzyme catalyzed processes.

If the free energy of transfer for the process $E_1 - M_1 \rightleftarrows E_2 - M_1$ is near zero, and all other transfers of metabolic intermediates, $E_l - M_i \rightleftarrows E_l + 1 - M_i$ (E_l is the last enzyme and M_i is the ith metabolite), are also of equal energy, metabolite transfer will be optimally facile throughout the pathway. Any preferential binding

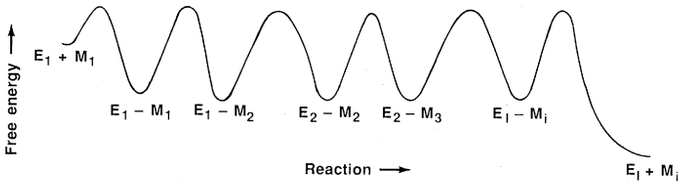

Fig. 4. Energetic consequences for the metabolite transfer. A hypothetical free energy diagram is shown for the sequence of enzyme catalyzed reactions, operating by the direct transfer of metabolites, throughout the pathway. E_I is the last enzyme, and M_i is the ith metabolite of the hypothetical metabolic pathway. Note, the equipartitions of substrate and product at individual enzyme sites, as well as the equipartitions of metabolites between adjacent enzyme sites.

of M_i by $E_l + 1$ versus E_l (presumably in the direction of the metabolic flow) will lead to either a higher activation energy barrier for internal reaction or to a less facile subsequent metabolite transfer. The free energy profile is illustrated for a hypothetical metabolic pathway in Fig. 3. To maintain this equipartition of energies in the transfer processes, and to optimize effective catalysis, the internal free energy change, $E_l - M_i \rightleftarrows E_l - M_i + 1$ must also evolve toward an internal equilibrium constant (K_{eq}^{int}) near unity.

This optimization of the facility for metabolite transfer by the direct transfer pathway demands that all of the intermediary metabolites of the metabolic pathway attain nearly equal concentrations within the physiological milieu. This prediction is in many instances far different from the predicted concentration ratios for intermediary metabolites restricted to an aqueous environment (*8, 21, 39*).

The argument that individual enzymes evolve to optimal catalytic efficiency, by matching the internal microscopic catalytic events to the bimolecular rates of association of substrate and product with enzyme, was proposed by Albery and Knowles (*40*). This argument is appropriate only for particular ranges of substrate and product concentrations in the aqueous environment, concentrations presumed to be physiologically relevant. As is evident from Table 1, the free aqueous concentrations can be far different from the total concentrations of intermediary metabolites in view of the high concentrations of high affinity enzyme sites and the low dissociability of enzyme substrate complexes. In the glycolytic pathway in muscle, the diffusion-controlled bimolecular associative reactions are not in general matched to the unimolecular internal transformation rates within the enzyme site.

The mechanism we propose, which also presumes that internal equilibrium constants are near unity for maximal efficiency, is based on enzyme-enzyme interaction and metabolite transfer as the regulating feature. An important distinction between the two models is that our model already assumes that transfer rates are modulated within an interactive system of enzymes and that efficiency develops by optimizing the interactions everywhere in the group of metabolically related enzymes. In contrast, the model of Albery and Knowles (*40*) includes the assumption that evolution proceeds via the optimization of catalytic efficiency of individual enzymes.

We might anticipate that if the last mentioned mechanism is correct, there would be some relation between catalytic reaction velocity and numbers of copies of particular enzymes within a metabolic pathway. Presumably, more efficient catalysts would be present in lower concentrations in order to optimize metabolic flux, and to minimize energy consumption because of excessive protein synthesis. The enzyme triose phosphate isomerase, for example, has the highest turnover number of all enzymes in the glycolytic pathway (Table 1). Nevertheless, it is present in substantially high concentrations, orders of magnitude higher than would be required for the optimal flux of metabolite through subsequent steps of catalysis (Table 1). A perusal of the concentrations of glycolytic enzymes in muscle and of the tricarboxylic acid cycle enzymes in the mitochondrial matrix precludes the expectation of balance between the relative catalytic efficiency of an enzyme and its number of catalytic sites in the cell (*41, 42*). Thus, it would appear that the glycolytic pathway has not been evolved for optimal catalytic rate with each individual enzyme. Rather, it appears that the system of enzymes function as a metabolic storehouse for the rapid interconversion between intermediary metabolites and final products. The unidirectional metabolic drive, according to our model of equal energy partitioning among enzyme-bound intermediates, arises because of the utilization of final product by another metabolic pathway or by export of the final product to a segregated location.

We have already demonstrated that sequential enzyme-enzyme interactions are determined by specific protein surface interactions (*34*). In a metabolic sequence proceeding entirely by way of the direct transfer mechanism, prior and subsequent enzyme-enzyme interactions necessarily perturb the particular enzyme-enzyme interacting pair. Hence, it is likely that the evolutionary optimization of metabolite transfer arises because of synergistic surface interactions throughout the pathway (*43*); changes in surface amino acid sequence everywhere in the pathway determine the compatibility of specific cognate enzyme pairs.

REFERENCES AND NOTES

1. D. K. Srivastava and S. A. Bernhard, *Curr. Top. Cell. Regul.* **28**, 1 (1986).
2. A. L. Lehninger, *Biochemistry* (Worth, New York, ed. 2, 1975).
3. D. E. Metzler, *Biochemistry, The Chemical Reactions of Living Cells* (Academic Press, New York, 1977).
4. G. Zubay, *Biochemistry* (Addison-Wesley, San Francisco, CA, 1983).
5. J. H. Ottaway and J. Mowbray, *Curr. Top. Cell. Regul.* **12**, 107 (1977).
6. H. R. Mahler and E. H. Cordes, *Biological Chemistry* (Harper & Row, New York, ed. 2, 1971).
7. P. A. Srere, *Science* **158**, 936 (1967).
8. ———, *Trends Biochem. Sci.* **9**, 387 (1984).
9. J. S. MacGregor *et al.*, *Proc. Natl. Acad. Sci. U.S.A.* 77, 3889 (1980).
10. G. R. Welch, *Prog. Biophys. Mol. Biol.* **32**, 103 (1977).
11. P. Friedrich, *Supramolecular Enzyme Organization* (Pergamon, Oxford, 1984).
12. P. A. Srere, in *Organized Multienzyme Systems*, G. R. Welch, Ed. (Academic Press, New York, 1985), pp. 1–61.
13. L. J. Reed and D. J. Cox, *Annu. Rev. Biochem.* **35**, 57 (1966).
14. A. Ginsburg and E. R. Stadtman, *ibid.* **39**, 429 (1970).
15. K. Kirschner and H. Bisswanger, *ibid.* **45**, 143 (1976).
16. E. W. Miles, *Adv. Enzymol. Relat. Areas Mol. Biol.* **49**, 127 (1979).
17. S. J. Wakil, J. K. Stoops, V. C. Joshi, *Annu. Rev. Biochem.* **52**, 537 (1983).
18. J. J. Volpe and P. R. Vagelos, *Physiol. Rev.* **56**, 339 (1976).
19. T. Shimakata and P. K. Stumpf, *Arch. Biochem. Biophys.* **217**, 144 (1982).
20. ———, *Plant Physiol.* **69**, 1257 (1982).
21. A. Sols and R. Marco, *Curr. Top. Cell. Regul.* **2**, 227 (1970).
22. R. H. Davis, in *Organizational Biosynthesis*, H. Vogel, J. O. Lampen, V. Bryson, Eds. (Academic Press, New York, 1967), pp. 303–322.
23. C. F. Cori, S. F. Velick, G. T. Cori, *Biochim. Biophys. Acta* **4**, 160 (1950).
24. A. P. Nygaard and W. J. Rutter, *Acta Chem. Scand.* **10**, 37 (1956).
25. D. K. Srivastava and S. A. Bernhard, *Biochemistry* **23**, 4538 (1984).
26. B. D. Nageswara RaO, M. Cohn, R. K. Scopes, *J. Biol. Chem.* **253**, 8056 (1978).
27. K. R. Huskins, thesis, University of Oregon, Eugene (1979).
28. ———, S. A. Bernhard, F. W. Dahlquist, *Biochemistry* **21**, 4180 (1982).
29. R. K. Scopes, in *The Enzymes*, P. D. Boyer, Ed. (Academic Press, New York, ed. 3, 1973), vol. 8, p. 335.
30. J. P. Weber and S. A. Bernhard, *Biochemistry* **21**, 4189 (1982).
31. D. K. Srivastava and S. A. Bernhard, *ibid.* **24**, 623 (1985).
32. K-S. You, *CRC Crit. Rev. Biochem.* 17, 313 (1984).
33. H. Simon and A. Kraus, in *Isotopes in Organic Chemistry*, E. Buncell and C. C. Lee, Eds. (Elsevier, Amsterdam, 1976), vol. 2, pp. 153–229.
34. D. K. Srivastava, S. A. Bernhard, R. Langridge, J. A. McClarin, *Biochemistry* **24**, 629 (1985).
35. D. K. Srivastava and S. A. Bernhard, *ibid.*, in press.
36. H. F. Fisher, D. L. Adija, D. G. Gross, *ibid.* **8**, 4224 (1969).
37. D. K. Srivistava and S. A. Bernhard, unpublished results.
38. J. R. Knowles, *Annu. Rev. Biochem.* **49**, 877 (1980).
39. R. L. Veech, J. W. R. Lawson, N. W. Cornell, H. A. Krebs, *J. Biol. Chem.* **254**, 6538 (1979).
40. W. J. Albery and J. R. Knowles, *Biochemistry* **15**, 5631 (1976).
41. R. Czok and T. Bucher, *Adv. Protein Chem.* **15**, 315 (1960).
42. D. Pette, in *Regulation of Metabolic Processes in Mitochondria*, J. M. Tagger, S. Papa, E. Quagliariello, E. C. Slater, Eds. (Elsevier, New York, 1966), pp. 28–48.
43. E. H. McConkey, *Proc. Natl. Acad. Sci. U.S.A.* **79**, 3236 (1982).

44. We thank Drs. D. E. Atkinson, J. R. Knowles, and L. E. Orgel for stimulating discussions during the preparation of this article. Supported by NIH grants GM10451 and GM37056 and by NSF grant PCM801-6249.